

# Polymeric nanoemulsions enriched with *Eucalyptus citriodora* essential oil

Flávia Oliveira Monteiro da Silva Abreu<sup>1\*</sup> , Emanuela Feitoza Costa<sup>1</sup>, Mayrla Rocha Lima Cardial<sup>1</sup> and Weibson Pinheiro Paz André<sup>2</sup>

<sup>1</sup>Laboratório Química Analítica e Química Ambiental – LAQAM, Programa de Pós-graduação em Ciências Naturais – PPGCN, Universidade Estadual do Ceará – UECE, Fortaleza, CE, Brasil

<sup>2</sup>Laboratório de Doenças Parasitárias – LABODOPAR, Programa de Pós-graduação em Ciências Veterinárias – PPGCV, Universidade Estadual do Ceará – UECE, Fortaleza, CE, Brasil

\*[flavia.monteiro@uece.br](mailto:flavia.monteiro@uece.br)

## Abstract

*Eucalyptus citriodora* oil has a well-known antimicrobial activity, however, its volatility limits its therapeutic applicability. Oil-in-water chitosan-based nanoemulsions have been prepared using a high-energy method in variable conditions in order to produce a stable formulation with an effective antimicrobial action. Physical-chemical characterizations and antimicrobial activity were performed. Results showed that the nanoemulsions with stability over 60 days and encapsulation efficiency higher than 90% were the ones with higher surfactant content. An optimal formulation was produced with the longer chain surfactant, which impacted in a particle size of  $489.2 \pm 0.25$  nm and encapsulation efficiency of  $92.5 \pm 0.17$ %. This formulation showed sustained release over 72h according to zero order kinetics, where the drug diffusion is lower than the respective dissolution release rate. The bactericidal action of the tested formulations showed an expressive inhibition rate against *S. typhimurium* (73%), with potential for an effective release system for antimicrobial control.

**Keywords:** chitosan, encapsulation, *Eucalyptus citriodora*.

**How to cite:** Abreu, F. O. M. S., Costa, E. F., Cardial, M. R. L., & André, W. P. P. (2020). Polymeric nanoemulsions enriched with *Eucalyptus citriodora* essential oil. *Polímeros: Ciência e Tecnologia*, 30(2), e2020024. <https://doi.org/10.1590/0104-1428.00920>

## 1. Introduction

The indiscriminate use of conventional antimicrobials has created resistant pathogens, which lead to the growth of severe infections and invasive diseases. Given this situation, research has been conducted in order to find alternative drugs. Plants are a rich source of pharmacologically interesting bioactive resources, and the antimicrobial potential of the Essential Oils (EO) has been explored in the last decade<sup>[1]</sup>. EOs are mixtures of chemical compounds that present aromatic structures of natural origin, where their constitution differs widely among plant species and is generally classified as terpenes, terpenoids and phenolic compounds<sup>[2]</sup>.

*Eucalyptus citriodora* belongs to the Myrtaceae family, and these species are known for the characteristics of their essential oils. It is known that the *E. citriodora* essential oil (ECEO) has a wide spectrum of biological activities, including herbicidal<sup>[3,4]</sup>, antifungal<sup>[5]</sup>, insecticide<sup>[6]</sup>, antioxidant<sup>[7,8]</sup>, antimicrobial<sup>[9,10]</sup> properties. However, the storage of EOs is a critical matter due to their sensitivity to heat, humidity and air, being subject to hydrolysis, oxidation, dehydration and isomerization reactions<sup>[11-13]</sup>. Thus, the encapsulation of EOs is an important nanotechnological strategy to enable the use of such constituents, improving their physical-chemical stability and promoting protection against external factors<sup>[14-18]</sup>.

Nanoemulsions (NEs) are useful alternatives in the encapsulation of EOs, enabling the improvement of physical-chemical stability, the modulation of release rates and bioavailability of such active principles, as it has been reported in recent studies<sup>[14-17]</sup>. The composition of the formulations, method and preparation conditions are intrinsically related, and it is necessary to conduct research to formulate more stable, efficient controlled release systems for the incorporation of active ingredients with antimicrobial action<sup>[12,14-18]</sup>.

Chitosan (Cs) is a cationic biopolymer in acid conditions, and is formed of D-glucosamine and N-acetyl-D-glucosamine bound by  $\beta$ -glycosidic bonds (1-4), it is a deacetylation of chitin, which is present in the shell of crustaceans<sup>[19]</sup>. Several studies have been carried out to explore its potential in different types of encapsulation matrices, such as nanoparticle systems<sup>[19,20]</sup>, nanogels<sup>[21,22]</sup>, nanoliposomes<sup>[9,23]</sup> conventional emulsions<sup>[24,25]</sup> and Pickering emulsions<sup>[26,27]</sup>. The use of Chitosan in a encapsulation system can enhance the transport of drugs across the nasal membrane, increasing the permeability of the epithelial membrane and retaining a formulation for extended time periods due to its mucoadhesive properties<sup>[16,20]</sup>. The addition of an anionic crosslinker into the chitosan-surfactant-oil

system may increase the nanoemulsion stability, in order to retain the oil inside the micelle for a longer time<sup>[14,20]</sup>. Although the effect of surfactant and oil relative content in nanoemulsions has been studied to some extent<sup>[19-22,25,26]</sup>, the main limitation of nanoemulsion system is caused by droplet growth and phase separation after a short period of time, which compromises the applicability. In this study, chitosan nanoemulsions incorporated with ECEO were developed adding a ionic crosslinker, aiming to improve the physical-chemical stability, statistically correlating the formulations conditions with the nanoemulsion stability aiming for antimicrobial applications.

## 2. Materials and Methods

### 2.1 Materials

The following materials were used: chitosan from shrimp (Cs) (Polymar, CE, 72% deacetylation degree,  $M_w = 3,3 \times 10^5 \text{ g.mol}^{-1}$ ), acetic acid (Dynamics). Nonionic surfactants Tween20® ( $T_{20}$ ) and Tween80® ( $T_{80}$ ) (Dynamics), Sodium Tripolyphosphate crosslinker agent (TPP) (Dynamics) and ECEO (FERQUIMA).

### 2.2 Preparation of nanoemulsion

Eight oil-in-water nanoemulsions (O/W) were prepared by means of the high-speed homogenization method, adapted from Ribeiro et al.<sup>[28]</sup>, by varying the type of the surfactant, and the relative content of Cs, ECEO and surfactant in the nanoemulsion. First, the surfactant agent (Tween 80 or Tween 20®) was added to ECEO at a mass ratio of 1:2 or 1:4 and then subjected to a vortex stirring (model NI1059 - Vortex) at 1000 rpm for 2 min, forming the oil phase. The oil phase was added to the Cs solution (1% v/v in acetic acid) to form the nanoemulsions with a volume ratio with the aid of a mechanical homogenizer Model ULTRA380 of the Ultrastirrer brand at 25.000 rpm over 2 min. The proportions 4:2 and 8:2 of the chitosan in relation to the ECEO were tested. A solution of ionic crosslinker agent TPP (0.5% m/v) was finally added in the system in the proportion chitosan:TPP 4:1 and 8:1 and then the mixture was kept under stirring for 1 min. About 200 ml of Nanoemulsions were produced, stored in close vials and kept in the refrigerator. A small portion of the nanoemulsions (10 ml) was frozen and then freeze-dried (L101, Liobras, Brazil) for FTIR and Scannin Electron Microscopy (SEM) analysis.

### 2.3 Experimental design and statistical analysis

A 2<sup>3</sup> replicate factorial design was performed to evaluate the influence of the factors in the efficiency of encapsulation of ECEO. Based on the literature and previous studies, the independent variables include the following factors: surfactant type (Tween 20 and 80, Factor A), quantitative ratio by chitosan and ECEO (4:2 and 8:2, factor B) and chitosan: surfactant ratio:TPP (4:1:1 and 8:1:1, Factor C). The dependent variables were the encapsulation efficiency of ECEO and viscosity. The factorial planning consisted of 8 experiments in replicate and the factors were evaluated at two different levels, low (-1) and high (+1), as described at Table 1. The statistical treatment of the data was

performed through ANOVA analysis in the Excel program (Microsoft 2013). The significance of the encapsulation parameters was verified using a confidence level of 95%, with a (p) value lower than 0.05.

### 2.4 Characterization of nanoemulsions

A physical stability study was carried out 24 hours, 30 days and 60 days after the preparation of the formulations, in order to verify visual signs of creaming or phase separation, adapted from Mwangi et al.<sup>[27]</sup> and Dickinson<sup>[29]</sup>, in closed vials, protected from light, kept at temperature of 26 °C. With the aid of a caliper, the thickness of the formed creaming was measured throughout the observation period. Creaming index (CI) was determined by measuring serum height ( $H_s$ ) and total height ( $H_t$ ) of an emulsion 1, 30 and 60 days after sample preparation, and calculated according to Equation 1<sup>[27]</sup>.

$$CI(\%) = \frac{H_s}{H_t} \times 100 \quad (1)$$

The viscosity of the emulsions was measured on an Ostwald type glass viscometer, timing the flow time. The viscosities of the samples were obtained through the calculation described by Almeida et al.<sup>[30]</sup>.

Particle size, polydispersity index (PDI) and zeta potential were determined after 30 days by dynamic light scattering using the Malvern Zetasizer equipment (Malvern Instruments, United Kingdom). The NE samples were dispersed in distilled water, forming a concentration of 0.1% (v/v) NE/water and left in agitation for 12 hours, to ensure full matrix dispersion in aqueous medium. The infrared spectra (FT-IR) were obtained using a Nicolet iS5 model spectrophotometer from Thermo Scientific. The samples were prepared in KBr tablets in the proportion 1:20 (m/m) (sample:KBr) and the spectra recorded in the range of 4000 to 400  $\text{cm}^{-1}$ , using 32 scans and 4  $\text{cm}^{-1}$  resolution.

### 2.5 Scanning electronic and optical microscopy

Morphological characterization was performed by SEM (Zeiss DSM, model 940A), using an accelerating voltage of 20kV and a magnification of 100-3000x. Samples were previously coated with platinum using a sputter coater (Electron Microscopy Sciences, Hatfield, PA, USA).

**Table 1.** Experimental conditions of Chitosan NPs production with *Eucalyptus citriodora* essential oil (ECEO).

Formulation code	Factor A Surfactant Type	Factor B Cs:ECEO Ratio	Factor C Cs:Surf:TPP Ratio
NE1	T <sub>20</sub>	4:2	4:1:1
NE2	T <sub>80</sub>	4:2	4:1:1
NE3	T <sub>20</sub>	8:2	4:1:1
NE4	T <sub>80</sub>	8:2	4:1:1
NE5	T <sub>20</sub>	4:2	8:1:1
NE6	T <sub>80</sub>	4:2	8:1:1
NE7	T <sub>20</sub>	8:2	8:1:1
NE8	T <sub>80</sub>	8:2	8:1:1

Factor A: Surfactant type: Tween 20 (-) and Tween 80 (+), Factor B: Cs:ECEO ratio: 4:2 (-) and 8:2 (+) and Factor C: Cs:Surfactant:Triphosphosphate (TPP) ratio:4:1:1 (-) and 8:1:1 (+).

Optical Microscopy was realized by placing 100  $\mu\text{L}$  of nanoemulsions between two glass lamins in an optical microscope (Digital OPTON- 40,model TNB-01-D) using an objective lens with 40x. Photos were acquired using a Software ISCapture using a magnification of 400x.

### 2.6 Encapsulation efficiency assessment

The quantity of encapsulated ECEO was adapted from Sugasini and Lokesh<sup>[31]</sup>. 1g of each nanoemulsion was sonicated for 10 minutes, diluted in ethanol (95%) in a 10 mL flask and centrifuged at 4000 rpm for 20 minutes. Subsequently, 1 mL of suspended material was removed and diluted with ethanol (96%) in a 5 mL flask and taken for reading in the Thermo Scientific Spectrophotometer (GENESYS 6 UV-Vis) at a wavelength of 214 nm.

The Encapsulation Efficiency (EE%) was calculated according to Equation 2:

$$EE(\%) = 100 \times \left( \frac{\text{Determined Oil Concentration}}{\text{Total Theoretical Oil Concentration}} \right) \quad (2)$$

It was prepared in triplicate in a standart solution of 500 ppm of ECEO in ethanol 96% (Dinamic). Further dilutions were made to obtain concentrations of 250, 210, 170, 130, 90, 80, 70, 60, 50, 40, 30, 20 and 10 mg.  $\text{L}^{-1}$ . The oil concentration was determined in the medium through a calibration curve, available in the Supplementary Material (Figure S1a), and represented by Equation 3:

$$Y = 0.0024x + 0.0615 \quad R^2 = 0.998 \quad (3)$$

### 2.7 Kinetic release profile

The most stable formulations were submitted to *in vitro* release tests. 300 mg of each sample was added in dialysis membranes (10 KDa) in a beaker containing 10 mL of distilled water at pH=7. Neutral pH was chosen to study the release in aqueous media, an environment where microorganisms present higher viability of action<sup>[32]</sup>. Aliquots of 3 mL were taken from the system at 15-minute intervals, in the first hour, and each 1 hour up to 8 hours, and after 24h and 72h. After each measurement, the aliquot was returned to the release system. A UV-vis spectrophotometer reading was performed at a wavelength of 214 nm and the concentration in the aqueous medium was converted using the calibration curve in water represented by Equation 4, available in the Supplementary Material (Figure S1b).

$$Y = 1.1631x + 0.0388 \quad R^2 = 0.981 \quad (4)$$

### 2.8 Antimicrobial activity

To standardize the technique and size of the inoculum, positive and negative gram bacteria were used, *Staphylococcus aureus* and *Salmonella typhimurium*, respectively, which were sown in 2 mL of the Trypticase Soy Agar (TSA) culture medium, after which they were placed in the incubator for 24 hours, before the test, for growing the microorganisms. An antimicrobial investigation was performed using the Müller Hinton agar diffusion method. The antimicrobial activity of NE was evaluated by using 100  $\mu\text{L}$  of NE and 30 cgm of Chloramphenicol as positive control. A negative control was made mixing chitosan, tween and TPP solution using

the same procedure as described for NE production, without the ECEO oil. Also, distilled water were used as negative control. The diameter of the inhibition zone was measured with a caliper up to the closest value of 0.1mm. The total area of the zone was calculated and subtracted from the disc area of the film and this difference in the area was reported as the inhibition zone.

## 3. Results and Discussions

### 3.1 Physico-chemical assessment of nanoemulsions

The effect of storage time on droplet size nanoemulsion was determined within 24 hours, 30 days and 60 days. The solubility of essential oils in an aqueous solution is higher than that of lipids composed of medium or long chain fatty acids<sup>[20]</sup>, therefore, nanoemulsions prepared from them are particularly prone to Ostwald maturation. During the analysis time, there was creaming formation for only two samples. The creaming rates in the respective time intervals of 24 hours, 30 days and 60 days are shown in Figure 1.

In the evaluation of the stability of the systems, the analysis of variance (ANOVA) (available in Supplementary Material, Table S1), revealed that the only significant factor is factor C, which studies the influence of the relative ratio between Cs: Surf:TPP. Thus, we can state that for the stability of the micellar system, the ratio between the Cs wall material, surfactant and TPP must be maintained at the relative ratio (4:1:1). It is observed that the first four formulations (T20QOT421, T80QOT421, T20QOT411 and T80QOT411), which were produced with a Cs:Surf 4:1 and Cs:TPP 4:1 ratio were more stable than the others, regarding the creaming and separation, because they had a percentage of segregated volume lower than 1%, even after 60 days.

During the interval of 24 hours, 30 and 60 days, the sample tests T<sub>20</sub>QOT841 and T<sub>20</sub>QOT821 were the only ones that presented a significant creaming formation, with values of 13.3% and 6.3%, respectively. These results were corroborated by the optical microscopy, where there was an increase of the droplets size in these formulations (available in Supplementary Material, Figure S2). It is observed that these samples were prepared with Tween 20 using a smaller amount of surfactant (Cs: Surf 8:1) and also lower TPP concentration, which lead to a relatively large emulsion droplets<sup>[27]</sup>. Phenomena related to the separation of phases of an emulsified system are linked to differences in density between the component phases of the system<sup>[29]</sup>, thus, it is possible to infer that the use of Tween 20 may have favored

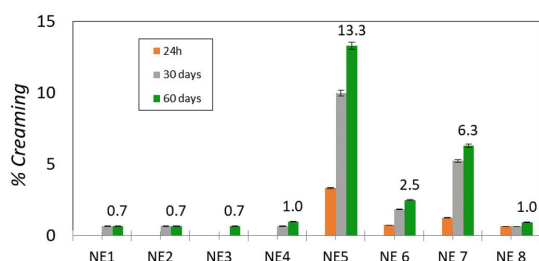


Figure 1. Creaming index at time intervals 24h, 30 and 60 days.

creaming in the mentioned compositions, since it is denser (1.1 g.cm<sup>-3</sup>) than Tween 80 (1.07 g.cm<sup>-3</sup>).

In the study of Mwangi et al.<sup>[27]</sup>, they investigated the effects of Cs concentration in Pickering emulsions and found that the increase in chitosan concentration from 0.01 to 0.3% w/v decreased the creaming rates, making it possible to consider that the polymer delayed the movement of the droplets. Xiong et al.<sup>[25]</sup> evaluated the addition of Cs in ovalbumin emulsions and reported that the increase in chitosan concentration (0.3% m/m) in the system considerably increased stability and decreased the formation of creaming. Calero et al.<sup>[33]</sup> observed that concentrations below 0.5% m/m of Cs tended to a significant increase in viscosity, which they attributed to the occurrence of flocculation of oil droplets and formation of creaming.

### 3.2 Encapsulation efficiency, zeta potential and particle size

Nanoemulsions presented considerable variation in the Encapsulation Efficiency values according to the reaction condition. Table 2 describes the values of Zeta Potential, Particle Size and Encapsulation Efficiency.

The nanoemulsions presented a content of ECEO that varied between approximately from 55 to 92%. The variance analysis (ANOVA) revealed that the significant factors were the relative ratio Cs/ECEO (factor B) and the relative ratio between Cs/Surfactant (factor C). Thus, we can state that for the stability of the micellar system, a greater oil retention capacity is obtained when the ratio between the wall material and the surfactant is maintained in the quantity (4:1) (NE1, NE2, NE3 and NE4). In the same way, the wall material must be in an optimum ratio of 4:2 in relation to the ECEO (NE1, NE2). In fact, the NE1 and NE2 formulations presented the highest encapsulation efficiency: 91.1 and 92.5, respectively. The data obtained showed that formulations in these proportions favored the occurrence of hydrophobic interactions between the essential oil constituents and the proposed matrix, leading to greater incorporation of the active ingredient.

In the study of Chitosan nanoparticles loaded with eugenol<sup>[34]</sup>, the highest encapsulation efficiency was achieved using the proportion Cs:eugenol of 1:1 using Tween 60 as surfactant. In another study, Chitosan nanoparticles loaded with carvacrol showed an ideal proportion of Cs:carvacrol 1:1 for an encapsulation efficiency of 31.4±1.3%<sup>[35]</sup>.

Regarding the effect of the variables on particle size, as shown in Table 2, nanoemulsions presented a droplet

diameter ranging from about 388 to 1271 nm, in agreement with the evaluated formulations. The ANOVA analysis revealed that the significant factors in particle size are factor A, which corresponds to the type of surfactant, and factor C, which studies the influence of the relative ratio between Cs:Surf:TPP. The relative amount of ECEO only showed significance when in interaction with the relative surfactant content. It was possible to show that a higher relative surfactant and higher TPP concentration amount in the formulation resulted in lower values of droplet diameters. Thus, we can state that the stability of the micellar system is achieved when Tween 80 is used with a higher relative amount and with higher relative amount of TPP (NE 2 and NE 4). When Tween 80 is used, smaller particle sizes are obtained, which means that there was less coalescence or lower degree of Ostwald maturation. At the same time, particles with increased size suffered from coalescence process, forming microemulsion instead of nanoemulsions, and caused an increase in the viscosity of the system<sup>[36]</sup>.

Viscosity ( $\eta$ ) is related to the colloidal stability of emulsified systems, where the lower the viscosity, the smaller the corresponding particle diameter, which in turn influences the inter-particle interactions<sup>[14]</sup>. The average viscosity of the NEs was 2.63 ±1.03 cP, and the formulations with relative content of Cs:Surf (4:1) presented significantly lower values of viscosity (NE1, NE2, NE3 and NE4), an indication of their stability. In this case, the effect related to a higher relative content of Tween in the formulation is observed, and there was a better solubilization of the oily phase to the surfactant. The surfactant was able to reduce the surface tension between the phases, influencing the reduction of the particle size, avoiding the coalescence process, and lower viscosity, consequently, promoting a single-phase system. The viscosity values as a function of the NE concentration are in Supplementary Material (Figure S3).

Regarding the zeta potential, all NEs presented high potential values (Table 2). The reduction of this potential leads to the reduction of electrostatic repulsion, facilitating the aggregation of particles, and is therefore used as an indication of the stability of a dispersion<sup>[37]</sup>. These positive values are a characteristic of an excellent electronic stabilization and are related to the protonated amino groups of Cs, which coat the micelles.

A schematic representation of the hypothetical structure for the micelle formed in the nanoemulsion are in Figure 2.

**Table 2.** Zeta Potential, Particle Size, Encapsulation Efficiency, Viscosity Results and Polidispersity Index (PDI).

	Formulation	Zeta Potential (mV)	Particle Size (nm)	Encapsulation Efficiency (%)	Viscosity (cP)	PDI	
	NE1	T20QOT421	+50.8±1.6	789±0.6	91.1±0.3	2.2 ±0.70	0.535± 0.02
	NE2	T80QOT421	+48.5±1.2	489±0.3	92.5±0.2	1.4±0.04	0.215 ± 0.03
	NE3	T20QOT411	+52.8±1.3	596±0.8	83.2±0.1	1.2±0.05	0.436 ± 0.03
	NE4	T80QOT411	+50.9±1.3	388±0.2	90.7±0.7	1.8±0.62	0.176 ± 0.01
	NE5	T20QOT841	+44.9±2.2	1248±1.2	73.9±1.1	3.4±0.92	0.684 ± 1.01
	NE6	T80QOT841	+40.7±1.9	921±0.9	69.3±0.9	3.3±0.97	0.687 ± 1.03
	NE7	T20QOT821	+31.0±2.7	1271±1.1	66.1±0.8	3.8±1.00	0.656± 1.01
	NE8	T80QOT821	+39.0±2.4	992±0.8	55.5±0.8	3.9±1.01	0.637± 1.00

The micelle is formed by ECEO in the central nucleus, stabilized by the surfactant. Chitosan entangles with the surfactant through intermolecular forces, coating the micelle. Finally, TPP is added and crosslink partially the chitosan network in order to increase the stability of the micelle.

### 3.3 Antimicrobial activity of NE formulations

Based on their higher stability, NE1, NE2, NE3 and NE4 were evaluated regarding their antimicrobial properties. Table 3 describes the antibacterial activity of nanoemulsions tested against *S. aureus* and *S. typhimurium* pathogens, where the chloramphenicol antibiotic was used as a positive control, distilled water and the NE1 Matrix and NE2 Matrix (without the ECEO oil) were used as a negative control.

**Table 3.** Antimicrobial activity of NE1, NE2, NE3 and NE4 tested against *S. aureus* and *S. typhimurium* pathogens.

Formulation	Inhibition Rate (%)	
	<i>S. Aureus</i>	<i>S. Typhimurium</i>
Chloramphenicol	100	100
OECO	21.8±4.9	23.7±1
NE 1 Matrix	22.8±2.2	21.4±1.4
NE 1	41.6±10.1	56.7±12.8
NE 2 Matrix	21.0±0.4	21.3±1.2
NE 2	55.6±10.0	73.2±13.3
NE 3	21.4±1.3	21.3±0.4
NE 4	23.4±3.9	21.9±3.6

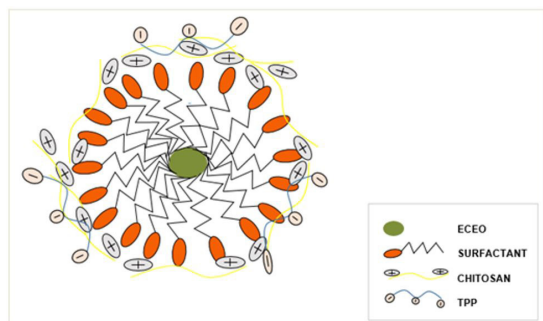


**Figure 2.** Schematic representation of the hypothetical structure for the micelle formed in the Cs-ECEO nanoemulsion.

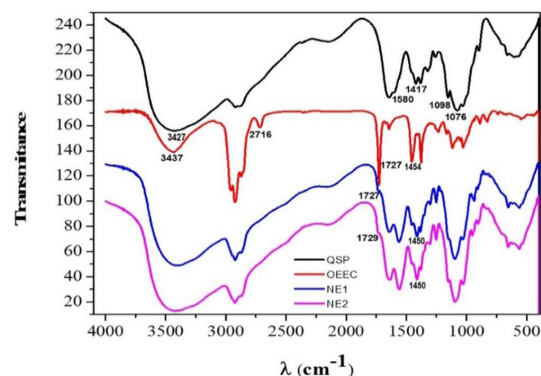


**Figure 3.** FTIR spectra of Chitosan, ECEO, NE1 (T20QOT421) and NE2 (T80QOT421).

NE1 and NE2 formulations showed an enhanced effect, with higher inhibitory activity when compared to the trial values with free ECEO, NE3, NE4 and the NE matrix. The NE1 formulation (T<sub>20</sub>QOT421) trial showed an inhibitory rate of 41.56% (10.37 mm) for *S. aureus* and 56.7% (13.61 mm) for *S. typhimurium*, versus the chloramphenicol inhibitory zone (25 mm). NE2 (T<sub>80</sub>QOT421) showed values of 55.6% for *S. aureus* (12.89 mm) and 73.32% (18.33 mm) for *S. typhimurium*. The OCEO free oil, which poses a known antimicrobial activity, with values of approximately 27% and 31% of inhibition rate against *S. aureus* and *S. typhimurium*, respectively.

On the other hand, NE3 and NE4 presented a discrete inhibition rate against *S. aureus* and *S. typhimurium*, with values close to those founded by NE matrices, around 21%. In this case, the antimicrobial activity is attributed to the chitosan matrix<sup>[38]</sup>. NE3 and NE4 presented lower ECEO content in the formulation in comparison with NE1 and NE2 (see Table 1), which probably caused the reduced effect. In this case, higher dosages would be required for NE3 and NE4 in order to achieve performance close to NE1 and NE2.

In this case, this is a clear indication that the proposed emulsification system optimizes the dispersibility of EO in aqueous solution and its physical-chemical stability increased its antimicrobial activity<sup>[39]</sup> and affirming that gram-positive bacteria are sensitive to plant derivatives, although they are more resistant due to their thick cell wall of peptidoglycan. On the other hand, an expressive inhibition rate against *S. typhimurium* of NE2 (T<sub>80</sub>QOT421) with 73.32% can be observed, being able to confirm that the concentration and type of surfactant favored the interaction of encapsulated essential oil with water, making it more available in the action on lipopolysaccharide membranes and their hydrophilic clusters found in gram-negative bacteria. In addition, the physical-chemical stability of the NE2 (T<sub>80</sub>QOT421) sample, as well as its reactive condition was ideal for inhibition activity for the tested microorganisms.

There are some reports in the literature that point to a strong search for evaluation of the antimicrobial activity of *Eucalyptus* plants and their various species<sup>[27,38-40]</sup>. The presence of *E. globulus* nanoemulsion incorporated with a relative content of 5% to chitosan films showed greater activity against *S. aureus* with an inhibition rate of 78.9%<sup>[38]</sup>.

Based on the encapsulation efficiency results and the inhibition rate, NE1 and NE2 were further characterized regarding their physico-chemical properties.

### 3.3 Absorption spectroscopy in the infrared region (FT-IR)

Figure 3 shows the infrared spectra (FT-IR) of Cs, ECEO and NE1 and NE2. Chitosan presents amine groups, which display broad stretching vibrations at 3,427 cm<sup>-1</sup>. The Cs main vibration modes are asymmetrical and symmetrical bending amine vibrations in 1580 and 1417 cm<sup>-1</sup>. The bands in 1092 cm<sup>-1</sup>, 1089 cm<sup>-1</sup> and 1093 cm<sup>-1</sup> are related to the C-O-C stretching of Cs<sup>[41]</sup>. On the other hand, a broadband centered on 3,437 cm<sup>-1</sup> is observed in the ECEO spectrum, referring to the O-H stretching modes of its alcoholic components, such as citronellol, isopulegol and neo-isopulegol<sup>[5]</sup>. These components are the main constituents of ECEO, as reported in the literature<sup>[42,43]</sup>. The strong-intensity narrow

band observed in  $1727\text{ cm}^{-1}$  and the medium-intensity band observed in  $1454\text{ cm}^{-1}$  for ECEO can be attributed, respectively, to the stretching of C=O and bending of C-H citronellal stretching mode<sup>[42]</sup>.

Despite the overlapping of the vibrational modes from Cs and ECEO around  $3,400\text{ cm}^{-1}$ , it was possible to observe the presence of citronellal component of the ECEO through the peaks in the region of  $1727$  and  $1724\text{ cm}^{-1}$  in the NE1 (T<sub>20</sub>QOT421) and NE2 (T<sub>80</sub>QOT421) formulations. NE1 and NE2 also showed a small peak at  $1450\text{ cm}^{-1}$ , due to the =C-H scissoring band present in citronellal and absent in Cs spectra, indicating the presence of ECEO major components incorporated in the NEs.

### 3.4 Morphology of nanoemulsions

The micrographs obtained by MEV of the NE2 are represented in the Supplementary Material (Figure S4). It was possible to observe the presence of microspherical inclusions as discrete particles, aggregated to the polymeric network, visualized in Figure S4a and S4b. NE2 presented a porous characteristic, with microspherical micellar domains embedded in the polymeric network, possibly caused by the increase of emulsion droplet during freeze drying process. In fact, the formation of porous structures in nanoemulsions has been attributed by the formation of micellar vacuoles in the polymeric network<sup>[44,45]</sup>. The addition of a cryoprotectant agent has been reported in the literature in order to preserve structural integrity and improve the shelf-life of nanoemulsions<sup>[44]</sup>.

### 3.5 Nanoemulsion *in vitro* release profile

The ECEO release kinetics of NE 1 (T20QOT421) and NE 2 (T80QOT421) are shown in Figure 4. The NE1 (T20QOT421) and NE2 (T80QOT421) formulations presented a similar release profile, in which they were constant in the first hours and gradually increased after 20 hours of study, with a controlled release profile. After 30 hours, it showed a more prolonged release profile with approximately 50% of oil released, reaching above 95% after 72 hours of release.

The release profile of the NEs was analyzed applying zero order, first order, Higuchi and Korsmeyer-Peppas kinetics<sup>[46]</sup>. Linear regression was used to calculate the values of the release constants (k) and the correlation coefficients (R<sup>2</sup>). Table 4 shows the correlation coefficients of the kinetic models for NE1 and NE2 samples.

NE 1 and NE2 showed that the *in vitro* release of ECEO was best fitted in the zero order kinetic model, due to the higher correlation coefficient (R<sup>2</sup>). This model is based on the slow release of the active substance from the emulsion system that gradually tend to disaggregate and disintegrate in the dissolution medium, where the drug diffusion speed, from the inside to the outside of the matrix, is lower than the respective dissolution speed<sup>[47]</sup>.

The release kinetics of the essential oil of *Pimenta dioica* presented a transport mechanism case II (zero order release kinetics) for chitosan/k carrageenan micro spheres (mass ratio 1:1) and a non-fickian release mechanism for chitosan/k-carrageenan micro spheres (1:0, 3:1 and 2:1). The release rate increased along with the chitosan content<sup>[48]</sup>.

**Table 4.** Determination coefficients (R<sup>2</sup>) for different kinetic models.

Model	Parameters	NE1	NE2
		T20QOT421	T80QOT421
Zero order	R <sup>2</sup>	0.9403	0.9391
	K <sub>0</sub> (h <sup>-1</sup> )	1.453	1.4351
First order	R <sup>2</sup>	0.8607	0.739
	K <sub>1</sub> (h <sup>-1</sup> )	0.0212	0.00226
Higuchi	R <sup>2</sup>	0.908	0.9348
	K <sub>H</sub> (h <sup>-1/2</sup> )	0.0538	0.0547
Korsmeyer-Peppas	R <sup>2</sup>	0.8177	0.8177
	K <sub>KP</sub> (h <sup>-n</sup> )	0.0144	0.0144

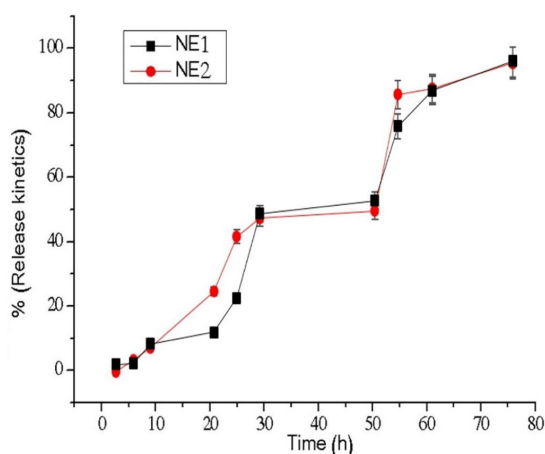


**Figure 4.** Release kinetics of ECEO for NE 1 (T20QOT421) e NE 2 (T80QOT421)

## 4. Conclusions

Chitosan Nanoemulsions enriched with *E. Citriodora* were produced, and the studied parameters presented a direct influence on the stability. Nanoemulsions with higher stability were the ones using Cs:Tween:TPP 4:1:1 mass ratio, with an average particle size of 565 nm, stable against creaming over 60 days of storage, verified visually and by optical microscopy. NE2 and NE1 presented the best set of properties, reaching an encapsulation efficiency value of 92.5% and significant inhibition rate against *S. aureus* and *S. typhimurium*., due to the chitosan: ECEO oil mass ratio of 4:2. Also, in these conditions, the type of surfactant influenced in relation to particle size, where Tween 80 provided smaller micellar sizes due to the enhanced solubilization of the oil phase, reducing the surface tension of the phases, implying directly in a lower particle size and lower viscosity. Kinetics showed a sustained release over three days, and the release profile best fitted were zero order kinetic model, corresponding to a slow release of the essential oil from the emulsion system that gradually disintegrate in the dissolution medium. Thus, we conclude that nanoemulsion of chitosan, tween and TPP enriched with *E. citriodora* were successfully optimized with potential for an effective release system for antimicrobial control.

## 5. Acknowledgements

The authors thank Professor Dra. Roselayne Ferro Furtado de Sá from Embrapa Agroindustria Tropical for SEM analysis. This work was supported by the Conselho Nacional de Desenvolvimento Científico - CNPq [Projeto Universal 442965/2014-1].

## 6. References

- Donsi, F., & Ferrari, G. (2016). Essential oil nanoemulsions as antimicrobial agents in food. *Journal of Biotechnology*, 233, 106-120. <http://dx.doi.org/10.1016/j.jbiotec.2016.07.005>. PMID:27416793.
- Semeniuc, C. A., Pop, C. R., & Rotar, A. M. (2017). Antibacterial activity and interactions of plant essential oil combinations against Gram-positive and Gram-negative bacteria. *Yao Wu Shi Pin Fen Xi*, 25(2), 403-408. <http://dx.doi.org/10.1016/j.jfda.2016.06.002>. PMID:28911683.
- Benchaa, S., Hazzit, M., & Abdelkrim, H. (2018). Allelopathic effect of *Eucalyptus citriodora* essential oil and its potential use as bioherbicide. *Chemistry & Biodiversity*, 15(8), e1800202. <http://dx.doi.org/10.1002/cbdv.201800202>. PMID:29893506.
- Khare, P., Srivastava, S., Nigam, N., Singh, A. K., & Singh, S. (2019). Impact of essential oils of *E. citriodora*, *O. basilicum* and *M. arvensis* on three different weeds and soil microbial activities. *Environmental Technology Innovation*, 14(4), 100343. <http://dx.doi.org/10.1016/j.eti.2019.100343>.
- Tolba, H., Moghrani, H., Benelmouffok, A., Kellou, D., & Maachi, R. (2015). Essential oil of Algerian *Eucalyptus citriodora*: chemical composition, antifungal activity. *Medical Mycology*, 25(4), e128-e133. <http://dx.doi.org/10.1016/j.mycmed.2015.10.009>. PMID:26597375.
- Bossou, A. D., Ahoussi, E., Ruysbergh, E., Adams, A., Smaghe, G., De Kimpe, N., Avlessi, F., Sohounhloue, D. C. K., & Mangelineckx, S. (2015). Characterization of volatile compounds from three *Cymbopogon* species and *Eucalyptus citriodora* from Benin and their insecticidal activities against *Tribolium castaneum*. *Industrial Crops and Products*, 76, 306-317. <http://dx.doi.org/10.1016/j.indcrop.2015.06.031>.
- Lin, L., Chen, W., Li, C., & Cui, H. (2019). Enhancing stability of *Eucalyptus citriodora* essential oil by solid nanoliposomes encapsulation. *Industrial Crops and Products*, 140, 111615. <http://dx.doi.org/10.1016/j.indcrop.2019.111615>.
- Singh, H. P., Kaur, S., Negi, K., Kumari, S., Saini, V., Batish, D. R., & Kohli, R. K. (2012). Assessment of *in vitro* antioxidant activity of essential oil of *Eucalyptus citriodora* (lemon-scented Eucalypt, Myrtaceae) and its major constituents. *Lebensmittel-Wissenschaft + Technologie*, 48(2), 237-241. <http://dx.doi.org/10.1016/j.lwt.2012.03.019>.
- Lin, L., Cui, H., Zhou, H., Zhang, X., Bortolini, C., Chen, M., Liu, L., & Dong, M. (2015). Nanoliposomes containing *Eucalyptus citriodora* as antibiotic with specific antimicrobial activity. *Chemical Communications*, 51(13), 2653-2655. <http://dx.doi.org/10.1039/C4CC09386K>. PMID:25573466.
- Paosen, S., Jindapol, S., Soontarach, R., & Voravuthikunchai, S. P. (2019). *Eucalyptus citriodora* leaf extract-mediated biosynthesis of silver nanoparticles: broad antimicrobial spectrum and mechanisms of action against hospital-acquired pathogens. *APMIS*, 127(12), 764-778. <http://dx.doi.org/10.1111/apm.12993>. PMID:31512767.
- Franz, C., & Novak, J. (2015). *Sources of essential oils*. Boca Raton: CRC Press. <http://dx.doi.org/10.1201/b19393-4>.
- Liu, Q., Zhang, M., Bhandari, B., Xu, J., & Yang, C. (2020). Effects of nanoemulsion-based active coatings with composite mixture of star anise essential oil, polylysine, and nisin on the quality and shelf life of ready-to-eat Yao meat products. *Food Control*, 107(33), 106771. <http://dx.doi.org/10.1016/j.foodcont.2019.106771>.
- Ryu, V., Corradini, M. G., Mclements, D. J., & Mclandsborough, L. (2019). Impact of ripening inhibitors on molecular transport of antimicrobial components from essential oil nanoemulsions. *Journal of Colloid and Interface Science*, 556, 568-576. <http://dx.doi.org/10.1016/j.jcis.2019.08.059>. PMID:31479830.
- Lovelyn, C., & Attama, A. A. (2011). Current state of nanoemulsions in drug delivery. *Journal of Biomaterials and Nanobiotechnology*, 2(5), 626-639. <http://dx.doi.org/10.4236/jbnb.2011.225075>.
- Majeed, H., Liu, F., Hategekimana, J., Sharif, H. R., Qi, J., Ali, B., Bian, Y.-Y., Ma, J., Yokoyama, W., & Zhong, F. (2016). Bactericidal action mechanism of negatively charged food grade clove oil nanoemulsions. *Food Chemistry*, 197(Pt A), 75-83. <http://dx.doi.org/10.1016/j.foodchem.2015.10.015>. PMID:26616926.
- Colombo, M., Figueiró, F., Fraga Dias, A., Teixeira, H. F., Battastini, A. M. O., & Koester, L. S. (2018). Kaempferol-loaded mucoadhesive nanoemulsion for intranasal administration reduces glioma growth *in vitro*. *International Journal of Pharmaceutics*, 543(1-2), 214-223. <http://dx.doi.org/10.1016/j.ijpharm.2018.03.055>. PMID:29605695.
- Ghosh, V., Mukherjee, A., & Chandrasekaran, N. (2013). Ultrasonic emulsification of food-grade nanoemulsion formulation and evaluation of its bactericidal activity. *Ultrasonics Sonochemistry*, 20(1), 338-344. <http://dx.doi.org/10.1016/j.ultsonch.2012.08.010>. PMID:22954686.
- Nirmal, N. P., Mereddy, R., Li, L., & Sultanbawa, Y. (2018). Formulation, characterisation and antibacterial activity of lemon myrtle and anise myrtle essential oil in water nanoemulsion. *Food Chemistry*, 254, 1-7. <http://dx.doi.org/10.1016/j.foodchem.2018.01.173>. PMID:29548427.
- Martins, A. F., de Oliveira, D. M., Pereira, A. G. B., Rubira, A. F., & Muniz, E. C. (2012). Chitosan/TPP microparticles obtained by microemulsion method applied in controlled release of heparin. *International Journal of Biological Macromolecules*, 51(5), 1127-1133. <http://dx.doi.org/10.1016/j.ijbiomac.2012.08.032>. PMID:22975304.
- Casettari, L., & Illum, L. (2014). Chitosan in nasal delivery systems for therapeutic drugs. *Journal of Controlled Release*, 190, 189-200. <http://dx.doi.org/10.1016/j.jconrel.2014.05.003>. PMID:24818769.
- Abreu, F. O. M. S., Oliveira, E. F., Paula, H. C. B., & Paula, R. C. M. (2012). Chitosan/cashew gum nanogels for essential oil encapsulation. *Carbohydrate Polymers*, 89(4), 1277-1282. <http://dx.doi.org/10.1016/j.carbpol.2012.04.048>. PMID:24750942.
- Beyki, M., Zhavah, S., Khalili, S. T., Rahmani-Cherati, T., Abollahi, A., Bayat, M., Tabatabaei, M., & Mohsenifar, A. (2014). Encapsulation of *Mentha piperita* essential oils in chitosan-cinnamic acid nanogel with enhanced antimicrobial activity against *Aspergillus flavus*. *Industrial Crops and Products*, 54, 310-319. <http://dx.doi.org/10.1016/j.indcrop.2014.01.033>.
- Dalmoro, A., Boichicchio, S., Nasibullin, S. F., Bertoncin, P., Lamberti, G., Barba, A. A., & Moustafine, R. I. (2018). Polymer-lipid hybrid nanoparticles as enhanced indomethacin delivery systems. *European Journal of Pharmaceutical Sciences*, 121, 16-28. <http://dx.doi.org/10.1016/j.ejps.2018.05.014>. PMID:29777855.
- Mutaliyeva, B., Grigoriev, D., Madybekova, G., Sharipova, A., Aidarova, S., Saparbekova, A., & Miller, R. (2017). Microencapsulation of insulin and its release using w/o/w double emulsion method. *Colloids and Surfaces A, Physicochemical and Engineering Aspects*, 521, 147-152. <http://dx.doi.org/10.1016/j.colsurfa.2016.10.041>.

25. Xiong, W., Ren, C., Tian, M., Yang, X., Li, J., & Li, B. (2018). Emulsion stability and dilatational viscoelasticity of ovalbumin/chitosan complexes at the oil-in-water interface. *Food Chemistry*, 252, 181-188. <http://dx.doi.org/10.1016/j.foodchem.2018.01.067>. PMID:29478530.
26. Shah, B. R., Zhang, C., Li, Y., & Li, B. (2016). Bioaccessibility and antioxidant activity of curcumin after encapsulated by nano and Pickering emulsion based on chitosan-tripolyphosphate nanoparticles. *Food Research International*, 89(Pt 1), 399-407. <http://dx.doi.org/10.1016/j.foodres.2016.08.022>. PMID:28460931.
27. Mwangi, W. W., Ho, K. W., Tey, B. T., & Chan, E. S. (2016). Effects of environmental factors on the physical stability of pickering-emulsions stabilized by chitosan particles. *Food Hydrocolloids*, 60, 543-550. <http://dx.doi.org/10.1016/j.foodhyd.2016.04.023>.
28. Ribeiro, J. C., Ribeiro, W. L. C., Camurça-Vasconcelos, A. L. F., Macedo, I. T. F., Santos, J. M. L., Paula, H. C. B., Araújo-Filho, J. V., Magalhães, R. D., & Bevilaqua, C. M. L. (2014). Efficacy of free and nanoencapsulated *Eucalyptus citriodora* essential oils on sheep gastrointestinal nematodes and toxicity for mice. *Veterinary Parasitology*, 204(3-4), 243-248. <http://dx.doi.org/10.1016/j.vetpar.2014.05.026>. PMID:24929446.
29. Dickinson, E. (2009). Hydrocolloids as emulsifiers and emulsions stabilizers. *Food Hydrocolloids*, 23(6), 1473-1482. <http://dx.doi.org/10.1016/j.foodhyd.2008.08.005>.
30. Almeida, A. C. S., Silva, J. P. M., Siqueira, A., & Frejlich, J. (1995). Medida de viscosidade pelo método de Ostwald: um experimento didático. *Revista Brasileira de Ensino de Física*, 17, 279-283. Retrieved in 2020, January 18, from <http://www.sbfisica.org.br/rbef/pdf/vol17a35.pdf>
31. Sugasini, D., & Lokesh, B. R. (2017). Curcumin and linseed oil co-delivered in phospholipid nanoemulsions enhances the levels of docosahexaenoic acid in serum and tissue lipids of rats. *Prostaglandins, Leukotrienes, and Essential Fatty Acids*, 119, 45-52. <http://dx.doi.org/10.1016/j.plefa.2017.03.007>. PMID:28410669.
32. Almajano, M. P., Carbó, R., Delgado, M. E., & Gordon, M. H. (2007). Effect of pH on the antimicrobial activity and oxidative stability of oil-in-water emulsions containing caffeic acid. *Journal of Food Science*, 72(5), C258-C263. <http://dx.doi.org/10.1111/j.1750-3841.2007.00387.x>. PMID:17995712.
33. Calero, N., Muñoz, J., Cox, P. W., Heuer, A., & Guerrero, A. (2013). Influence of chitosan concentration on the stability, microstructure and rheological properties of O/W emulsions formulated with high-oleic sunflower oil and potato protein. *Food Hydrocolloids*, 30(1), 152-162. <http://dx.doi.org/10.1016/j.foodhyd.2012.05.004>.
34. Woranuch, S., & Yoksan, R. (2013). Eugenol-loaded chitosan nanoparticles: I. thermal stability improvement of eugenol through encapsulation. *Carbohydrate Polymers*, 96(2), 578-585. <http://dx.doi.org/10.1016/j.carbpol.2012.08.117>. PMID:23768603.
35. Keawchaon, L., & Yoksan, R. (2011). Preparation, characterization and *in vitro* release study of carvacrol-loaded chitosan nanoparticles. *Colloids and Surfaces. B, Biointerfaces*, 84(1), 163-171. <http://dx.doi.org/10.1016/j.colsurfb.2010.12.031>. PMID:21296562.
36. Sing, A. J. F., Graciaa, A., Lachaise, J., Brochette, P., & Salager, J. L. (1999). Interactions and coalescence of nanodroplets in translucent O/W emulsions. *Colloids and Surfaces A, Physicochemical and Engineering Aspects*, 152(1-2), 31-39. [http://dx.doi.org/10.1016/S0927-7757\(98\)00622-0](http://dx.doi.org/10.1016/S0927-7757(98)00622-0).
37. Katata-Seru, L., Lebepe, T. C., Aremu, O. S., & Bahadur, I. (2017). Application of Taguchi method to optimize garlic essential oil nanoemulsions. *Journal of Molecular Liquids*, 244, 279-284. <http://dx.doi.org/10.1016/j.molliq.2017.09.007>.
38. Hafsa, J., Smach, M. A., Ben Khedher, M. R., Charfeddine, B., Limem, K., Majdoub, H., & Rouatbi, S. (2016). Physical, antioxidant and antimicrobial properties of chitosan films containing *Eucalyptus globulus* essential oil. *Lebensmittel-Wissenschaft + Technologie*, 68, 356-364. <http://dx.doi.org/10.1016/j.lwt.2015.12.050>.
39. Shakeri, A., Khakdan, F., Soheili, V., Sahebkar, A., Rassam, G., & Asili, J. (2014). Chemical composition, antibacterial activity, and cytotoxicity of essential oil from *Nepeta ucrainica* L. spp. *kopetdagensis*. *Industrial Crops and Products*, 58, 315-321. <http://dx.doi.org/10.1016/j.indcrop.2014.04.009>.
40. Knezevic, P., Aleksic, V., Simin, N., Svircev, E., Petrovic, A., & Mimica-Dukic, N. (2016). Antimicrobial activity of *Eucalyptus camaldulensis* essential oils and their interactions with conventional antimicrobial agents against multi-drug resistant *Acinetobacter baumannii*. *Journal of Ethnopharmacology*, 178, 125-136. <http://dx.doi.org/10.1016/j.jep.2015.12.008>. PMID:26671210.
41. Tang, D. W., Yu, S. H., Ho, Y. C., Huang, B. Q., Tsai, G. J., Hsieh, H. Y., Sung, H. W., & Mi, F. L. (2013). Characterization of tea catechins-loaded nanoparticles prepared from chitosan and an edible polypeptide. *Food Hydrocolloids*, 30(1), 33-41. <http://dx.doi.org/10.1016/j.foodhyd.2012.04.014>.
42. Araújo-Filho, J. V., Ribeiro, W. L. C., André, W. P. P., Cavalcante, G. S., Guerra, M. C. M., Muniz, C. R., Macedo, I. T. F., Rondon, F. C. M., Bevilaqua, C. M. L., & Oliveira, L. M. B. (2018). Effects of *Eucalyptus citriodora* essential oil and its major component, citronellal, on *Haemonchus contortus* isolates susceptible and resistant to synthetic anthelmintics. *Industrial Crops and Products*, 124, 294-299. <http://dx.doi.org/10.1016/j.indcrop.2018.07.059>.
43. Farag, N. F., El-Ahmady, S. H., Abdelrahman, E. H., Naumann, A., Schulz, H., Azzam, S., & El-Kashoury, E. S. A. (2018). Characterization of essential oils from Myrtaceae species using ATR-IR vibrational spectroscopy coupled to chemometrics. *Industrial Crops and Products*, 124, 870-877. <http://dx.doi.org/10.1016/j.indcrop.2018.07.066>.
44. Morais, A. R. V., Alencar, É. N., Xavier, Jr., F. H., Oliveira, C. M., Marcelino, H. R., Barratt, G., Fessi, H., Egitto, E. S. T., & Elaissari, A. (2016). Freeze-drying of emulsified systems: a review. *International Journal of Pharmaceutics*, 503(1-2), 102-114. <http://dx.doi.org/10.1016/j.ijpharm.2016.02.047>. PMID:26943974.
45. Fernandes, R. V. D. B., Borges, S. V., & Botrel, D. A. (2014). Gum arabic/starch/maltodextrin/inulin as wall materials on the microencapsulation of rosemary essential oil. *Carbohydrate Polymers*, 101, 524-532. <http://dx.doi.org/10.1016/j.carbpol.2013.09.083>. PMID:24299808.
46. Dash, S., Murthy, P. N., Nath, L., & Chowdhury, P. (2010). Kinetic modeling on drug release from controlled drug delivery systems. *Acta Poloniae Pharmaceutica Drug Research*, 67(3), 217-223. PMID:20524422.
47. Lopes, C. M., Lobo, J. M. S., & Costa, P. (2005). Formas farmacêuticas de liberação modificada: polímeros hidrofílicos. *Revista Brasileira de Ciências Farmacêuticas*, 41(2), 143-154. <http://dx.doi.org/10.1590/S1516-93322005000200003>.
48. Dima, C., Cotârlet, M., Alexe, P., & Dima, S. (2014). Reprint of "Microencapsulation of essential oil of pimento [*Pimenta dioica* (L) Merr.] by chitosan/k-carrageenan complex coacervation method". *Innovative Food Science & Emerging Technologies*, 25, 97-105. <http://dx.doi.org/10.1016/j.ifset.2014.07.008>.

Received: Jan. 18, 2020

Revised: July 28, 2020

Accepted: July 30, 2020



## **Supplementary Material**

Supplementary material accompanies this paper.

Figure S1: Calibration curves (a) in Ethanol; (b) in water with surfactant.

Table S1: ANOVA Statistic Results of influence on the parameters on Creaming.

Figure S2: Optical Microscopy of Emulsion droplets for NEs a) NE1; b) NE2; c) NE3 and d) NE4 after 30 days (a, b, c, d) and after 60 days (a', b', c' d').

Figure S3: Viscosity of NEs as a function of the concentration.

Figure S4. Scanning Electron Microscopy surface images of NE 2 (T80QOT421) at different magnification a) 667x and b) 2670x.

This material is available as part of the online article from <http://www.scielo.br/po>

## Polymeric nanoemulsions enriched with *Eucalyptus citriodora* essential oil

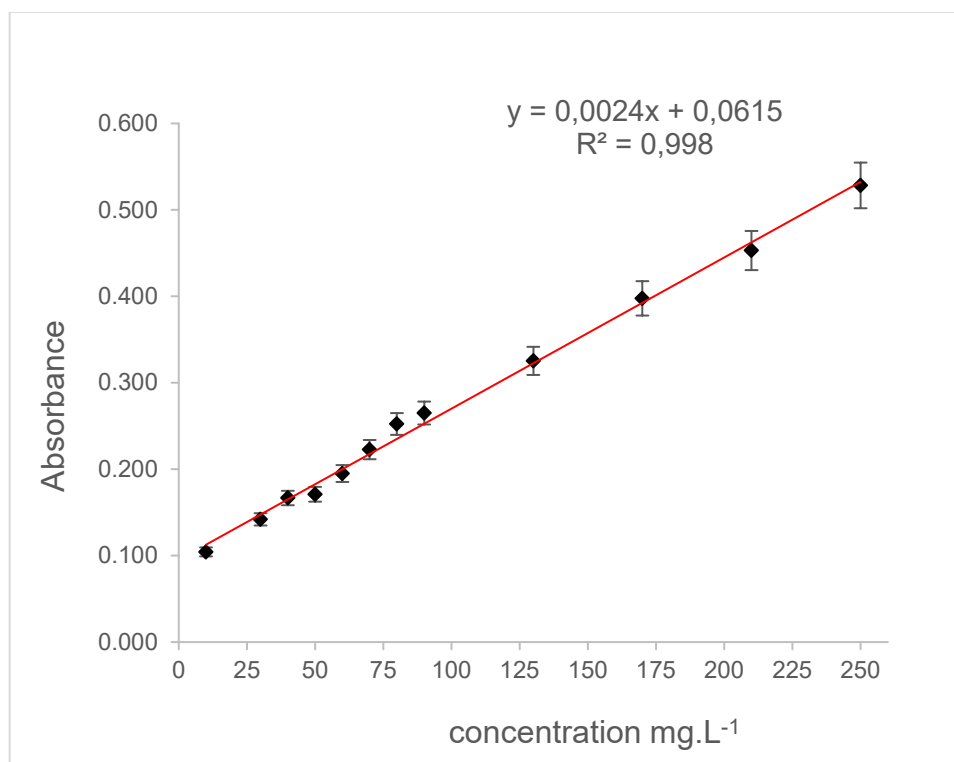
Flávia Oliveira Monteiro da Silva Abreu<sup>1\*#</sup>, Emanuela Feitoza Costa<sup>1</sup>, Mayrla Rocha Lima Cardial<sup>1</sup> and Weibson Pinheiro Paz André<sup>2</sup>

*1 Laboratório Química Analítica e Química Ambiental – LAQAM, Programa de Pós-graduação em Ciências Naturais – PPGCN, Universidade Estadual do Ceará - UECE, 60740-000, Fortaleza, CE, Brazil*

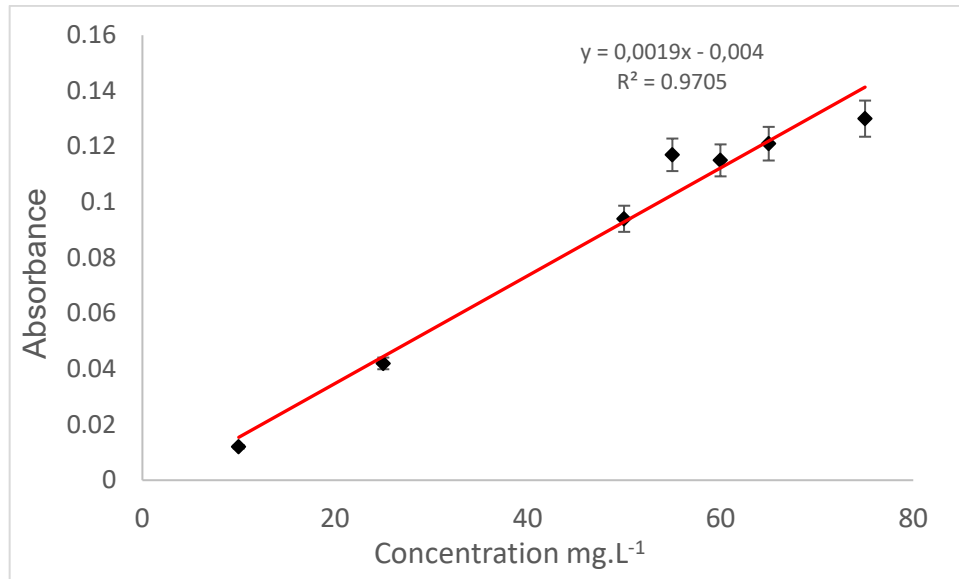
*2 Laboratório de Doenças Parasitárias – LABODOPAR, Programa de Pós-graduação em Ciências Veterinárias – PPGCV, Universidade Estadual do Ceará – UECE, 60740-000, Fortaleza, CE, Brazil*

\*flavia.monteiro@uece.br

#<https://orcid.org/0000-0003-4759-2739>



(a)



(b)

Figure S1: Calibration curves (a) in Ethanol; (b) in water with surfactant.

Table S1: ANOVA Statistic Results of influence on the parameters on Creaming.

	<b>SQ</b>	<b>GL</b>	<b>MQ</b>	<b>Fo</b>	<b>Fcritical</b>
<b>SQA</b>	31.21	1	31,2	4,862	
<b>SQB</b>	8.41				
<b>SQC</b>	50.00	1	50,0	7,79	7,71
<b>SQAB</b>	4.21				
<b>SQAC</b>	33.62	1	33,6	5,239	
<b>SQBC</b>	9.68				
<b>SQABC</b>	3.38				
<b>Sqerror</b>	25.67	4	6,4		
<b>SQTotal</b>	140.50	7			

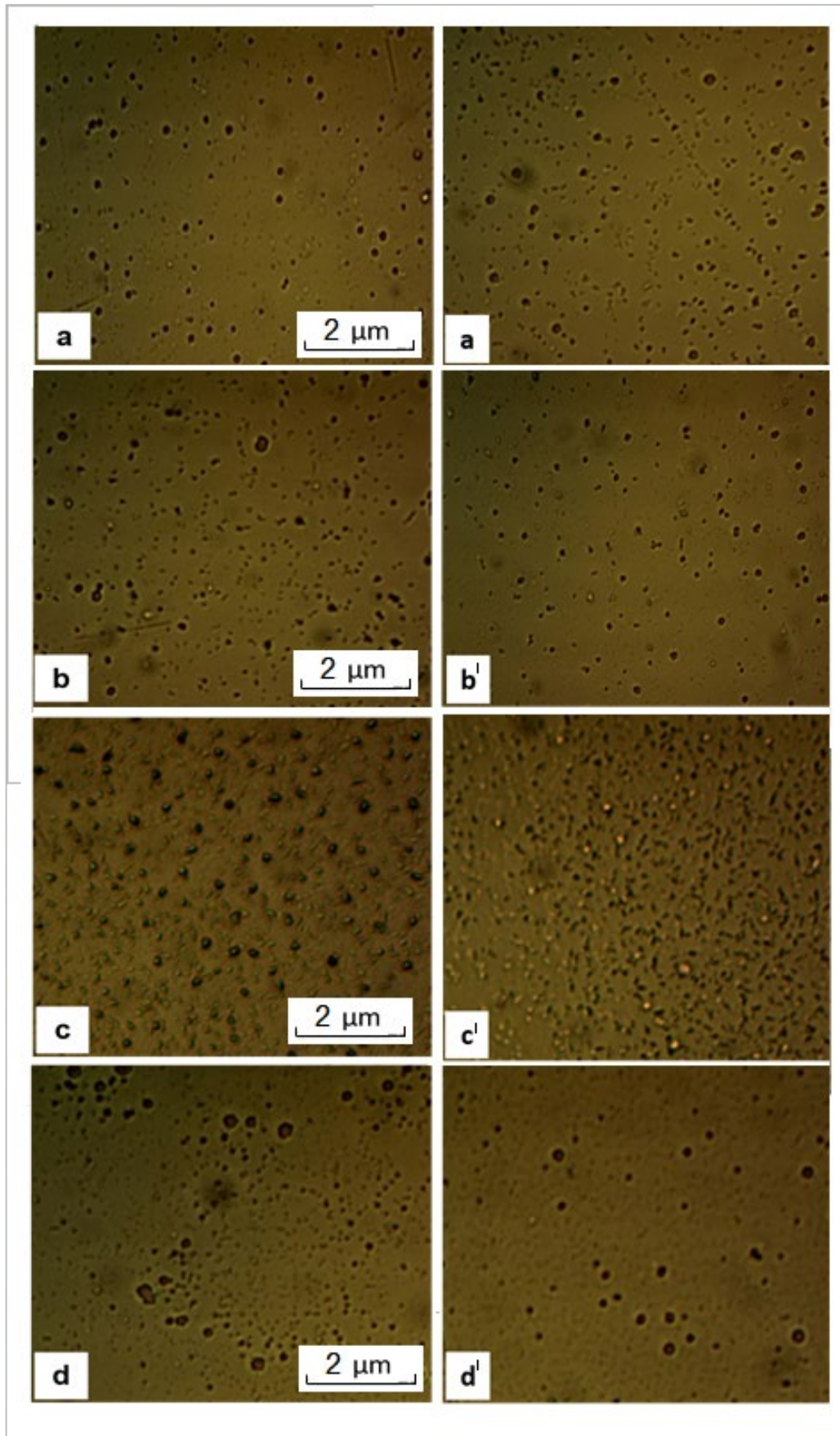


Figure S2: Optical Microscopy of Emulsion droplets for NEs a) NE1; b) NE2; c) NE3 and d) NE4 after 30 days (a, b, c, d) and after 60 days (a', b', c' d' ).

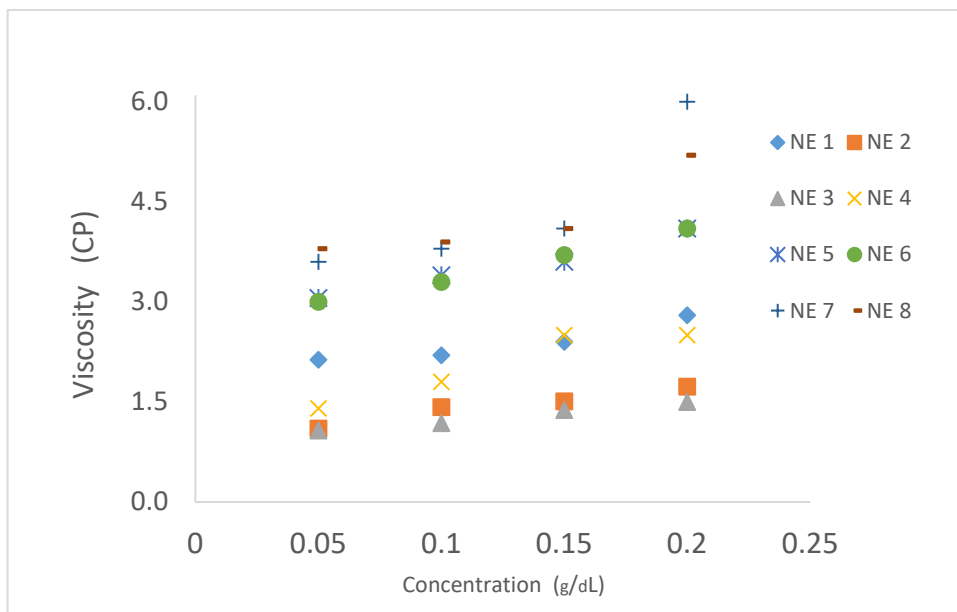


Figure S3: Viscosity of NEs as a function of the concentration.

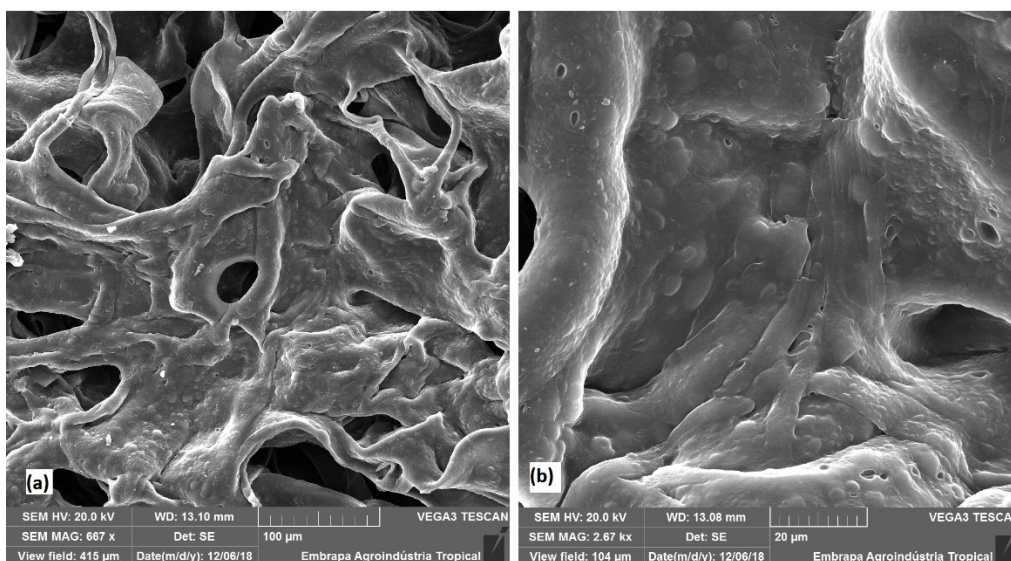


Figure S4. Scanning Electron Microscopy surface images of NE 2 (T80QOT421) at different magnification a) 667x and b) 2670x.